



PCCP

**Efficiency Maximization in Solar-Thermochemical Fuel  
Production: Challenging the Concept of Isothermal Water  
Splitting**

Journal:	<i>Physical Chemistry Chemical Physics</i>
Manuscript ID:	CP-ART-03-2014-000978
Article Type:	Paper
Date Submitted by the Author:	07-Mar-2014
Complete List of Authors:	Ermanoski, Ivan; Sandia National Laboratories, Miller, James E.; Sandia National Laboratories, Allendorf, Mark; Sandia National Laboratory,

SCHOLARONE™  
Manuscripts

# Efficiency Maximization in Solar-Thermochemical Fuel Production: Challenging the Concept of Isothermal Water Splitting

I. Ermanoski<sup>a</sup>, J. E. Miller<sup>a</sup>, M. D. Allendorf<sup>b</sup>

<sup>a</sup>Sandia National Laboratories, Albuquerque, NM 87185

<sup>b</sup>Sandia National Laboratories, Livermore, CA 94551-0969

## Abstract

Widespread adoption of solar-thermochemical fuel production depends on its economic viability, largely driven by the efficiency of use of the available solar resource. Herein, we analyze the efficiency of two-step cycles for thermochemical hydrogen production, with emphasis on efficiency. Owing to water thermodynamics, isothermal H<sub>2</sub> production is shown to be impractical and inefficient, irrespective of reactor design or reactive oxide properties, but an optimal temperature difference between cycle steps, for which efficiency is the highest, can be determined for a wide range of other operating parameters. A combination of well-targeted pressure and temperature swing, rather than either individually, emerges as the most efficient mode of operation of a two-step thermochemical cycle for solar fuel production.

## 1. Introduction

Solar fuel production has the potential to dramatically change the world's energy posture: from the prospecting and extraction of today, to renewable production using sunlight and atmospheric gases in the future. The issue in solar fuel production is not one of mere feasibility, as this can be accomplished via multiple pathways (e.g. thermochemical, electrochemical, even biological), but one of practical economic viability, expressed via metrics such as the levelized fuel cost, which is strongly tied to efficiency.

Two-step thermochemical fuel production processes are a conceptually simple and promising approach: a working material (oxide) is partially or fully reduced at a high temperature, then cooled and, in the case of water splitting, exposed to steam to be reoxidized and yield H<sub>2</sub>. The reduction to practice of these theoretically efficient processes has, however, been challenging.<sup>1</sup> Existing working materials, for example, have a low reversible oxygen capacity, yielding little H<sub>2</sub> per mole oxide per cycle. The large energy requirement for heating the reactive material between cycle steps necessitates solid-solid heat recovery at high temperature. Also, maximizing the per-cycle yield drives operation to very low thermal reduction pressures and very high thermal reduction temperatures. The former require large vacuum pumps or high-purity sweep gasses, and the latter lead to excessive aperture radiation losses and require the use of specialized materials.

The current work was motivated by the understanding that the cost of solar collection is a dominant overall cost factor for solar fuels in general, and for specifically proposed thermochemistry-based system designs.<sup>2,3</sup> The implications of these and similar studies are that efforts should focus on researching and designing for efficiency and ease of operation. It is therefore of substantial importance for further progress in this field to develop methods for determining the operating and design parameter space that maximize efficiency, given a reactor type and working material properties.

The broad question of reactor efficiency has been examined in detail by Siegel et al., arriving at the concept of the utilization coefficient as an indicator of achievable efficiency for a reactor/material combination in a two-step thermochemical cycle.<sup>4</sup> In a recent analysis Miller et

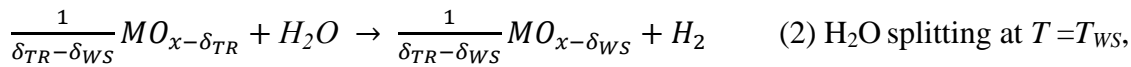
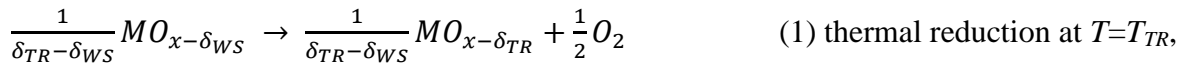
al. addresses efficiency from an even broader thermodynamic viewpoint, and establish a framework for materials design.<sup>5</sup>

In this work we search for a prescription for maximizing efficiency from the reactor design and operation point of view. We consider two specific, yet important situations. Firstly, we analyze the special case of isothermal water splitting (ITWS) in a two-step water splitting cycle, because the analysis is completely independent of reactive material properties or reactor design, making the results the most generally applicable. ITWS is also of added interest, having been recently suggested by several groups as possibly advantageous compared to temperature swing water splitting (TSWS).<sup>6-8</sup> The results of this part of the analysis present a map of the relevant operation parameter space, and the challenges in implementing the isothermal concept.

To address the subject of maximizing efficiency, including the comparison between isothermal and temperature-swing operation, we analyze a two-step metal oxide reactor that uses ceria as a working oxide to produce H<sub>2</sub> from H<sub>2</sub>O.<sup>9</sup> Even though the results are somewhat specific, important generalizations can be made, especially with respect to optimal reactor temperatures, and prospective reactive oxide materials. Thermodynamic similarities between water and CO<sub>2</sub> splitting give confidence that the results and conclusions would be similar.

## 2. Approach

**2.1 General thermodynamic considerations** Reactions (1) and (2) below, which sum to give reaction (3), generically describe a two-step thermochemical cycle for H<sub>2</sub>O splitting based on a reactive metal oxide. Reaction (1) is an endothermic thermal reduction of the metal oxide carried out at a temperature,  $T_{TR}$ . After removal of the evolved oxygen the reduced oxide reacts mildly exothermically with H<sub>2</sub>O at temperature  $T_{WS}$  to yield H<sub>2</sub> via reaction (2), and is restored to its original state, ideally for indefinite reuse. The net result, reaction (3), is the splitting of H<sub>2</sub>O (with separate recovery of H<sub>2</sub> and O<sub>2</sub>) driven by thermal energy:



Here,  $\delta_{TR}$  and  $\delta_{WS}$  are the extents of reduction of the oxide, following the thermal reduction and water splitting steps. Their difference,  $\Delta\delta = \delta_{TR} - \delta_{WS}$ , is the reversible oxygen capacity, as realized in the cycle. The oxygen partial pressure for the reduction reaction is  $p_{O_2}$ .

At any temperature the Gibbs free energies of the above reactions add up:

$$\Delta G_1^\circ = \Delta G_3^\circ - \Delta G_2^\circ \quad (4),$$

meaning that reactions (1) and (2) are thermodynamically spontaneous only in distinct and non-intersecting regions, i.e.  $\Delta G_1^\circ(T_{TR}), \Delta G_2^\circ(T_{WS}) < 0$  only for  $\Delta T = T_{TR} - T_{WS} > 0$ . If the cycle is carried out in these temperature regions, it is driven entirely by thermal energy, i.e. a primary heat source. However, cyclically heating and cooling the oxide between  $T_{TR}$  and  $T_{WS}$  opens the possibility for thermal losses that may render H<sub>2</sub> production inefficient in practice.

At temperatures where reactions (1) and (2) are not spontaneous, additional energy must be provided to the system (generally in some form other than heat, i.e. a secondary energy source) in order to drive the reactions towards the same endpoints. The minimum amount of thermal energy,  $Q_{min}$  that must be supplied to carry out the cycle in this general case is:

$$Q_{min}(T_{TR}, T_{WS}) = \Delta H_1^\circ(T_{TR}) + \frac{(1-\varepsilon_R)}{\Delta \delta F_R} C_p \Delta T + \frac{\Delta G_1^\circ(T_{TR})}{\eta_1} + \frac{\Delta G_2^\circ(T_{WS})}{\eta_2} \quad (5).$$

The 1<sup>st</sup> term on the right-hand side is simply the reduction endotherm. The 2<sup>nd</sup> term accounts for thermal cycling, where  $C_p$  is the molar specific heat capacity of the reactive oxide,  $F_R$  is the molar fraction of the solid that is reactive (as opposed to inert), and  $\varepsilon_R$  is the effectiveness of solid-solid heat recovery. The 3<sup>rd</sup> and 4<sup>th</sup> terms generically (the process is not specified) account for the scenario(s) where reactions (1) and/or (2) are carried out at unfavorable temperatures, i.e. when  $\Delta G_1^\circ(T_{TR}) > 0$  and/or  $\Delta G_2^\circ(T_{WS}) > 0$ , and represent the minimum work must be performed to drive reaction (1) and/or (2). This work is determined by  $\Delta G_1^\circ$  and/or  $\Delta G_2^\circ$  at the respective conditions. Coefficients  $\eta_1$  and  $\eta_2$  account for losses in converting heat to the required amount of work. Additionally, they implicitly include the possibility that waste heat (i.e. heat of reoxidation and unrecovered oxide sensible heat) can be used to provide part of the work in the 3<sup>rd</sup> and 4<sup>th</sup> term. (See also discussion of eq. 11.) The limiting case ( $Q_{min} = \Delta H_1^\circ$ ) applies to a system operating in the favorable temperature regimes with ideal heat recovery ( $\varepsilon_R = 1$ ).

To understand the implications of eq. 5, consider the situation where  $\Delta T = 0$  (ITWS), at a temperature intermediate to those of the thermodynamically favorable regimes. In this case, no energy is required for thermal cycling (the 2<sup>nd</sup> term is zero), but work must be added to both reactions (1) and (2). As  $T_{TR} = T_{WS}$  change in value, the 2<sup>nd</sup> term remains zero and  $\Delta G_1^\circ$  and  $\Delta G_2^\circ$  increase and decrease in opposition to one another. As shown in Section 3.1, the thermodynamic limits of this special case can be determined without any knowledge of the reactor design or properties of the working materials.

More interestingly, from an application perspective, if  $T_{TR}$  is increased and  $T_{WS}$  is decreased to realize TSWS, the thermal cycling energy requirement (2<sup>nd</sup> term) becomes nonzero and grows, but the work requirements embodied by  $\Delta G_1^\circ$  and  $\Delta G_2^\circ$  decrease and are eventually eliminated. Thus, eq. 5 suggests that for a given material (defining the thermodynamics) and set of reactor and process designs (defining the various efficiencies, practical and physical limitations, parasitic losses, etc.) there should be such  $T_{TR}$  and  $T_{WS}$ , that minimize the sum of the last three terms in eq. 5, and therefore  $Q_{min}$ .

## 2.2 Reactive oxide thermodynamics, reactor model, and efficiency definitions

Determining the conditions under which a two-step reactor operates at maximum efficiency requires knowledge of the thermodynamic properties of the working material, as well as a reactor model. Specific thermodynamic properties of reactive oxides are not generally known, and are typically determined by extensive experimentation.<sup>10-19</sup> Generalizations can therefore be made, but there is no universal solution.

For the purpose of efficiency calculations, we assume  $\text{CeO}_2$  as the active oxide, a well-characterized candidate material for solar-thermochemical water splitting. The thermodynamics of  $\text{CeO}_2$  are obtained from the work of Zinkevich et al.<sup>20</sup> These authors performed a comprehensive, critical review of the thermodynamic literature concerning cerium oxides and applied a Calphad analysis to derive models covering all relevant phases (including both liquids and solids).<sup>21</sup> This comprehensive approach covers the entire temperature range relevant to our analysis, and is necessary to accurately describe non-stoichiometric phases, such as the ceria fluorite phase ( $\text{CeO}_{2-\delta}$ ) of concern here, which persists from  $\delta = 0$  to  $\delta \approx 0.3$  at 1773 K.<sup>20</sup> This model also generally predicts lower values of  $\delta(p, T)$  than models based solely on the experiments by Panlener<sup>10</sup>, used in almost all previous studies.<sup>13-16, 19</sup> This difference leads to

lower overall efficiency predictions for the comprehensive approach, but does not change the conclusions of the analysis. The difference between ceria reduction models is illustrated in Fig. 3 in the next section.

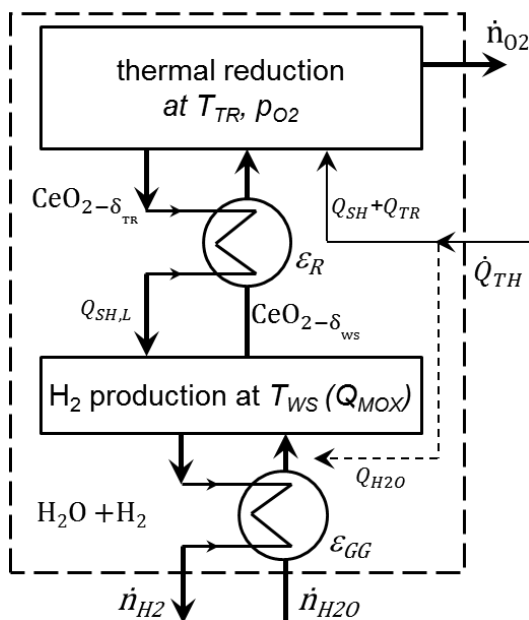


Figure 1. Reactor schematics. Heat exchangers and their effectiveness ( $\epsilon_R$  and  $\epsilon_{GG}$ ) are indicated in the oxide and steam flows. The input solar heat power  $\dot{Q}_{TH}$  is used to add sensible heat to the ceria ( $Q_{SH}$ ) and to partially reduce it ( $Q_{TR}$ ). If the combined heat from the  $H_2$  production reaction ( $Q_{MOX}$ ) and the unrecovered sensible heat of the oxide ( $Q_{SH,L}$ ), is insufficient to heat steam to  $T_{WS}$  ( $Q_{H2O}$ ), part of  $\dot{Q}_{TH}$  is used. For simplicity and because it is of minor importance, heat recovery from the  $O_2$  stream is not shown, but it is included in the calculations (cf. eq. 11).

The reactor, schematically illustrated in Fig. 1, is assumed to accomplish four primary unit operations, common to many thermochemical reactor designs. These are a thermal reduction, solid-solid heat recovery in a recuperator,  $H_2$  production (water splitting), and a steam pre-heating.<sup>9</sup> During operation, concentrated solar radiation heats and thermally reduces the reactive oxide in a thermal reduction chamber. The oxide then moves through the recuperator (entering at the hot inlet) and then into an  $H_2$  production chamber, where it is exposed to a pre-heated steam flow in a countercurrent arrangement, producing  $H_2$ . The reoxidized material is then brought back to the reduction chamber, via the recuperator, where heat is exchanged between the two oxide flows.

The reactor *heat-to- $H_2$  efficiency* or *reactor efficiency*,  $\eta_R$ , is defined as:

$$\eta_R = \frac{\dot{n}_{H_2} HHV_{H_2}}{\dot{Q}_A} \quad (6),$$

where  $\dot{n}_{H_2}$  is the hydrogen molar production rate,  $HHV_{H_2}$  is its higher heating value, and  $\dot{Q}_A$  is the solar power at the reactor aperture. Efficiency calculations incorporate an important assumption: *Only solar primary energy is used for the entire operation of the reactor.* This includes all heat needs, such as thermal reduction, ceria and feedstock heating, and heat equivalents of mechanical work, such as vacuum pumping, compression, oxide moving, etc. Equally importantly, all major losses and inefficiencies are also included, (e.g. black body

radiation through the aperture at a concentration ratio  $C_A=3000$ , conversion efficiency from heat to mechanical work, etc.) Radiation losses are included in the reactor efficiency for completeness and for ease of comparison with other work. The sensible heat of the product gasses is used to preheat steam (with a gas-gas heat recovery effectiveness  $\varepsilon_{GG}$ ), and to generate power. Conduction losses through insulated reactor walls are considered negligible in a large device. The sensible heat in the  $O_2$  product is comparatively small, and its omission or inclusion has little effect on the efficiency calculations.<sup>9</sup>

The  $H_2$  molar production rate in eq. 6 can be expressed in terms of the heat input power ( $\dot{Q}_{TH}$ ) and the heat required for production of 1 mol  $H_2$  ( $Q_{mol}$ ):

$$\dot{n}_{H_2} = \frac{\dot{Q}_{TH}}{Q_{mol}} \quad (7).$$

After losses to aperture intercept ( $A=0.95$ ) and thermal re-radiation ( $P_{rad}$ ),  $\dot{Q}_{TH}$  can be expressed as:

$$\dot{Q}_{TH} = A * \dot{Q}_A - P_{rad} \quad (8),$$

whereas  $Q_{mol}$  is:

$$Q_{mol} = Q_{TR} + Q_{SH} + Q_{AUX} \quad (9).$$

Here the individual terms (roughly ordered by decreasing temperature) correspond to those in eq. 5 as follows:  $Q_{TR}=\Delta H_r(\text{CeO}_2)$  is the thermal reduction endotherm. The energy required for heating the oxide (sensible heat) from  $T_{WS}$  to  $T_{TR}$  (assuming  $F_R=1$ ) is:

$$Q_{SH} = \frac{C_p}{\Delta\delta} \Delta T (1 - \varepsilon_R) \quad (10),$$

where the molar heat capacity of  $\text{CeO}_2$  is  $C_p \approx 80 \text{ J/mol K}$ .<sup>22</sup> Finally,  $Q_{AUX}$  encompasses the heat equivalents of other, auxiliary, energy requirements:

$$Q_{AUX} = (Q_{H_2O} + Q_{pump} + Q_{mech} + Q_{sep}) - (Q_{MOX} + Q_{SH,L} + Q_{O_2}) \quad (11).$$

Here  $Q_{H_2O}$  is the energy required to heat steam by  $\Delta T_{I/O}=T_{WS}-T_0$ , i.e. from ambient temperature ( $T_0$ ) to  $T_{WS}$ , and it includes preheating by hot product streams. The heat equivalents of the pumping of products (in both chambers) and mechanical and separation work are  $Q_{pump}$ ,  $Q_{mech}$ , and  $Q_{sep}$ , respectively. The negative terms represent the waste heat available from the product gasses, mainly the  $H_2O-H_2$  mix, which consists of the heat released at  $T_{WS}$  in the reoxidation reaction,  $Q_{MOX}=\Delta H_r - \Delta H_c^0_{H_2}$ , and the unrecovered sensible heat of the oxide,  $Q_{SH,L}$ . Steam, in the fuel production chamber, acts as both a reactant (oxidizer) and a coolant. The sensible heat in the oxygen exhaust is  $Q_{O_2}$ .

Importantly,  $Q_{AUX}$  is forced to be non-negative, i.e. it is set to zero when the waste heat exceeds the first three terms in eq. 11, since heat at  $T_{WS}$  cannot contribute to either  $Q_{TR}$  or  $Q_{SH}$ . The quantities in eq. 11 are heat equivalents, so conversion efficiency terms are included where applicable, such as the conversion of heat to mechanical or pump work. An efficiency of 10% was used for heat-to-pump work and for the oxide moving work. Thermal reduction and water splitting are assumed to end in their thermodynamic equilibrium states, i.e. kinetic limitations are not considered.

### 3. Results

**3.1 Isothermal water splitting** The appeal of ITWS lies in the perceived simplification of reactor design and operation, as it eliminates the need for solid-solid heat recovery and, depending on the design, the frequent temperature cycling of reactor components.

Coincidentally, this special case lends itself to straightforward theoretical analysis. To begin, we use well-known relationships for each of the reactions (1), (2), and (3):

$$\Delta G^\circ = -RT \ln K \quad \text{and} \quad \Delta G^\circ = \Delta H^\circ - T\Delta S^\circ \quad (12) \text{ and } (13),$$

where  $R$  is the gas constant. The equilibrium constants for reactions (1) and (2) depend on the reactant and product activities:

$$K_1 = \frac{(a_{O_2})^{1/2}(a_{MO_{x-\delta_{TR}}})^{1/\Delta\delta}}{(a_{MO_{x-\delta_{WS}}})^{1/\Delta\delta}} \quad \text{and} \quad K_2 = \frac{(a_{H_2})(a_{MO_{x-\delta_{WS}}})^{1/\Delta\delta}}{(a_{H_2O})(a_{MO_{x-\delta_{TR}}})^{1/\Delta\delta}} \quad (14) \text{ and } (15).$$

At all relevant operating pressures, the gas activities can be expressed as partial pressures:

$$a_{O_2} = p_{O_2} \quad \text{and} \quad \frac{a_{H_2}}{a_{H_2O}} = \frac{p_{H_2}}{p_{H_2O}} \quad (16) \text{ and } (17),$$

where  $p_{O_2}$  is measured relative to standard pressure. Substituting eqs. 12, 13, 16 and 17 into eq. 4 gives:

$$\begin{aligned} -RT_{iso} \ln(p_{O_2}^{1/2}) - RT_{iso} \ln\left(\frac{a_{MO_{x-\delta_{TR}}}}{a_{MO_{x-\delta_{WS}}}}\right)^{1/\Delta\delta} &= \Delta H_3^\circ - T_{iso}\Delta S_3^\circ + RT_{iso} \ln\left(\frac{p_{H_2}}{p_{H_2O}}\right) + \\ &+ RT_{iso} \ln\left(\frac{a_{MO_{x-\delta_{WS}}}}{a_{MO_{x-\delta_{TR}}}}\right)^{1/\Delta\delta} \quad (18). \end{aligned}$$

Here  $T_{iso}$ , is the isothermal operating temperature. Solving for  $T_{iso}$  is facilitated by the exact cancellation of the oxide terms on the left and right side of eq. 18, giving:

$$T_{iso} = \frac{-\Delta H_3^\circ}{R\left(\ln(p_{O_2}^{1/2}) - \ln\left(\frac{p_{H_2O}}{p_{H_2}}\right)\right) - \Delta S_3^\circ} \quad (19).$$

In Fig. 2a, based on eq. 19, we graphically show the relationship between  $T_{iso}(n_{w/h})$ , and  $p_{O_2}$  ( $n_{w/h}=n_{H_2O}/n_{H_2}$  in the oxidation step; ideal gas behavior is assumed so  $p_{H_2O}/p_{H_2}$  and  $n_{H_2O}/n_{H_2}$  are used interchangeably). It is evident from the figure that relaxing one parameter results in the restriction of one or both of the other two. For example, decreasing  $T_{iso}$  requires either a  $p_{O_2}$  decrease or an  $n_{w/h}$  increase, or both. Importantly, Fig. 2a strictly applies to an *ideal isotherma cycle*. A real isothermal cycle would require even more stringent operating conditions than an ideal one (e.g. a higher  $T_{iso}$  at the same values of  $p_{O_2}$  and  $n_{w/h}$ ), for example due to kinetic limitations.

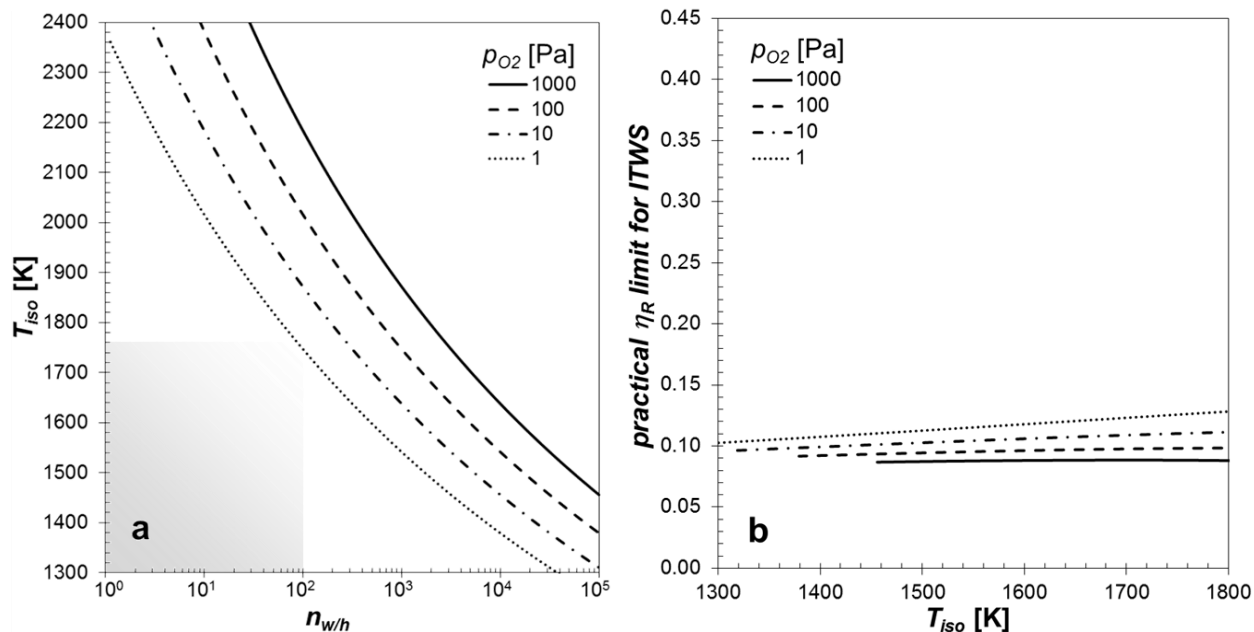


Figure 2. (a) Relationship between  $T_{iso}(n_{w/h})$  and  $p_{O_2}$ . For the water splitting reaction constant thermodynamic values of  $\Delta H_3^\circ = 250.8 \frac{\text{kJ}}{\text{mol}}$  and  $\Delta S_3^\circ = 57.35 \frac{\text{J}}{\text{mol-K}}$  are assumed. These are the values at 1673 K and best represent the temperature range of practical interest. Adopting values for a different temperature introduces very small differences in the results. The fading rectangle in (a) roughly indicates a reasonable operating parameter space for a practical reactor and shows that ITWS largely falls outside of it. (b) Practical efficiency limits for ITWS. Efficiency curves are plotted for  $n_{w/h} < 10^5$ . The lack of results below certain  $T_{iso}$  for the higher  $p_{O_2}$  values indicates that ITWS is not possible for  $n_{w/h} < 10^5$ . The efficiency scale in (b) was chosen for ease of comparison with Figs. 3, 4 and 5.

It is important to understand that the results in Fig. 2a are general in the sense that a cycle represented by a valid combination of the three parameters can be performed by multiple possible materials, which must satisfy eq. 4 at  $T_{iso}$ . Conversely, this requirement means that an isothermal cycle, defined by a point in the graph, cannot be realized by arbitrarily chosen materials.

The high temperatures (in this case  $T_{TR} = T_{WS} = T_{iso}$ ), low  $p_{O_2}$ , and high  $n_{w/h}$  values indicated in Fig. 2a, raise questions regarding the ultimate feasibility of ITWS. To understand the implications of these results and to outline a realistic space of operating parameters, we consider the practical limitations regarding  $T_{TR}$ ,  $p_{O_2}$ , and  $n_{w/h}$ .

Increasing  $T_{iso}$  corresponds to less strict  $p_{O_2}$  (higher) and  $n_{w/h}$  (lower) requirements, and isothermal temperatures as high as 2173 K have been considered.<sup>6, 7</sup> However, radiation losses through the reactor aperture, as well as oxide sublimation and reactivity with reactor structures, limit  $T_{TR}$  to no more than 1773 K in devices of practical relevance.<sup>5</sup> To appreciate the challenge of ITWS under the extreme conditions considered in the literature,<sup>6, 7</sup> it is instructive to note that at 2173 K, ceria has a vapor pressure  $p_{CeO_2} \approx 9.3$  Pa,<sup>23</sup> leading to a swift and irreversible oxide loss via sublimation, as observed experimentally by Abanades et al.<sup>24</sup>

We assume that low  $p_{O_2}$  is achieved by pumping, i.e. lowering of  $p_{TR}$ , the total pressure in this step (therefore  $p_{O_2} = p_{TR}$ ). As shown in a previous analysis,<sup>9</sup> the heat equivalent of pump work is not a major contributor to the total energy requirement, but the lowest  $p_{TR}$  is limited by other factors, such as oxygen volumetric flow and entering the molecular flow regime, to no less than 1 Pa.

The alternative, isothermal inert gas sweeping, was examined by Bader et al.<sup>6</sup>, who showed that, even under best-case conditions, the amount of required N<sub>2</sub> by far exceeds the amount of the H<sub>2</sub> product ( $n_{N_2}/n_{H_2} \approx 700$ ). In addition to requiring an N<sub>2</sub> purification plant, the only manner of somewhat efficient ITWS was found to require exceptionally high levels of heat recovery (>95%) between the incoming and outgoing N<sub>2</sub> gas – at  $T_{iso}$ . Finally, the vast majority of the products are the inert-oxygen mix and steam, not H<sub>2</sub>. We therefore do not consider sweeping an option for ITWS.

The above practical limitations regarding  $T_{TR}$  and  $p_{TR}$  give context to the results in Fig. 2a: For example, even for very low  $p_{TR}$  (e.g. 1 Pa), and the highest operationally relevant  $T_{iso}$  of 1773 K, large amounts of steam must be provided for a very low H<sub>2</sub> yield ( $n_{h/w} = n_{H_2}/n_{H_2O} \ll 1$ ); i.e. the majority of the reactor “product” would then be unreacted steam, not H<sub>2</sub>. In short, ITWS requires impractically high thermal reduction temperatures, or exceptionally low thermal reduction pressures, or results in an exceptionally low H<sub>2</sub> fraction in the output stream. As the derivation of eq. 19 shows, these results and associated limitations are a consequence of water thermodynamics and the basic relationship for the Gibbs free energy of the reduction and oxidation reactions (eq. 4), and can therefore not be circumvented by either redox material choice or innovative reactor design.

For a deeper insight into the implications of the tradeoffs associated with ITWS, the low H<sub>2</sub> fraction or high  $n_{w/h}$  values can be viewed in the context of separation work, i.e. the work that must be performed to separate H<sub>2</sub> from the H<sub>2</sub>-poor output stream. Separation work is directly related to efficiency, and practical ITWS efficiency limits, as defined in eq. 6, can be estimated by including some well-established efficiencies of the constituent processes. Re-radiation losses are given in eq. 8 ( $\sim T_{iso}^4$ ). Separation work (2<sup>nd</sup> law) depends on  $T_{iso}$ ,  $n_{h/w}$ , and the final H<sub>2</sub> purity, assumed here to be a modest  $x_{H_2} = 99.9\%$ . The practical separation efficiency (i.e. theoretical 2<sup>nd</sup> law work vs. actual work) is generally  $\sim 15\%$ , albeit not at the high temperatures considered here.<sup>25</sup> The heat-to-power efficiency of a Rankine cycle in concentrated solar power plants, necessary to perform pump and separation work, is at best  $\approx 40\%$ . Finally, neglecting other work and heat requirements, and keeping the assumption for the heat-to-pumping efficiency (10%) from Section 2.2, we plot in Fig. 2b the practical limits for ITWS efficiency ( $\eta_R$ ).

The results show that the ITWS  $\eta_R$  values are low, even at high  $T_{iso}$  and low  $p_{O_2}$ . The limits are almost independent of  $T_{iso}$  and depend very weakly on  $p_{O_2}$ . In light of the outstanding operating conditions shown in Fig. 2a, low efficiencies should not be surprising. The relative insensitivity of the results on  $T_{iso}$  and  $p_{O_2}$  may, on the other hand, be initially unexpected. This, however, is a manifestation of the mutual dependence of the operating conditions ( $p_{O_2}$ ,  $n_{w/h}$ , and  $T_{iso}$ ), which are dictated solely by water thermodynamics as expressed in eq. 19. Simply put, the results in Fig. 2b show that, whether one in practice accepts higher re-radiation losses (to increase  $T_{iso}$ ), or chooses to invest work in pumping (to lower  $p_{O_2}$ ) or in H<sub>2</sub> separation (to allow higher  $n_{w/h}$ ), the overall ITWS efficiency limit is roughly the same, in what can be viewed as a thermodynamic zero-sum game.

**3.2 Maximizing Efficiency** The above results describe the conditions required for ITWS and indicate the practical difficulties in realizing it, including inherent efficiency limitations. In this section, we examine the effects of operational parameters on efficiency in the general case where  $\Delta T \geq 0$ . In this case, we must include both material and reactor assumptions, as detailed in section 2.2. We limit  $p_{TR}$  to values between 1 Pa and 1 kPa - low enough to meaningfully facilitate

thermal reduction, but not too low to be entirely unfeasible in a reactor in the field. Likewise, we set  $T_{TR}=1773$  K.

To begin, in Fig. 3 we show the efficiency  $\eta_R(p_{TR})$ , for several values of  $\Delta T$ ,  $\varepsilon_R=0.5$ , and  $\varepsilon_{GG}=0.8$ . Two important features are immediately evident in the plot. Firstly, ITWS ( $\Delta T=0$ ) yields the lowest efficiency for every  $p_{TR}$  in the range. Secondly, for  $p_{TR}\approx 75$  Pa and above, ITWS efficiency is zero, whereas TSWS ( $\Delta T>0$ ) for the same  $p_{TR}$  yields a positive efficiency.

The latter is a special case of a more general result, also evident in Fig. 3: for low values of  $\Delta T$ , the efficiency is zero above some critical  $p_{TR}$ . This stems from the presence of oxygen in steam as a result of partial dissociation, characterized by a well-known pressure,  $p_{O_2,d}$  (e.g.  $p_{O_2,d}(1773\text{ K})\approx 75$  Pa). For some values of  $p_{TR}$  and  $T_{WS}$ , the equilibrium oxygen pressure above the oxide,  $p_{O_2,ceO_2-\delta_{TR}}(T_{WS})$ , exceeds  $p_{O_2,d}(T_{WS})$ , leading to further oxide reduction (not reoxidation) in steam, and yielding no  $H_2$  product.

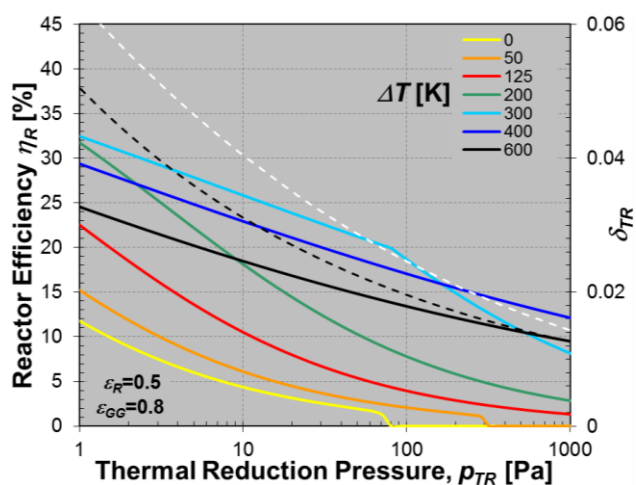


Figure 3. Solid lines show the calculated reactor efficiency as function of  $p_{TR}$ , for several values of  $\Delta T$  (left y-axis). Note the nil efficiency for ITWS above  $p_{TR}\approx 75$  Pa, and the initial efficiency increase, followed by a decrease, as  $\Delta T$  increases from 0 K to 400 K. Dashed lines, on the right y-axis, show the extent of thermal reduction,  $\delta_{TR}$  (assuming  $T_{TR}=1773$  K). The black dashed line is for the comprehensive model used in this work (based on Zinkevich et al.<sup>20</sup>), whereas the white line is based on Panlener<sup>10</sup> only.

We now aim to determine  $\Delta T_{opt}$ , defined as the value of  $\Delta T(p_{TR}, \varepsilon_R, \varepsilon_{GG})$  for which  $Q_{min}$  (eq. 5) is the smallest, and efficiency ( $\eta_R$ ) is the highest. To visually introduce the  $\Delta T_{opt}$  concept, we invite the reader to follow the efficiency curves in Fig. 3, from yellow to black, at a constant  $p_{TR}$ . A trend is evident:  $\eta_R(\Delta T)$  initially increases and then decreases with  $\Delta T$ . Focusing on this trend, we show in Fig. 4 the efficiency as function of  $\Delta T$ ,  $\eta_R(\Delta T)$ , for  $\varepsilon_R=0$  and  $\varepsilon_R=0.75$ , with two values of  $\varepsilon_{GG}$  (0.8 and 0.6) and several values of  $p_{TR}$ . The chosen values for  $\varepsilon_R$  and  $\varepsilon_{GG}$  reflect the awareness that heat recovery at high temperature is challenging, and a high effectiveness, however desirable, may not be possible in practice.

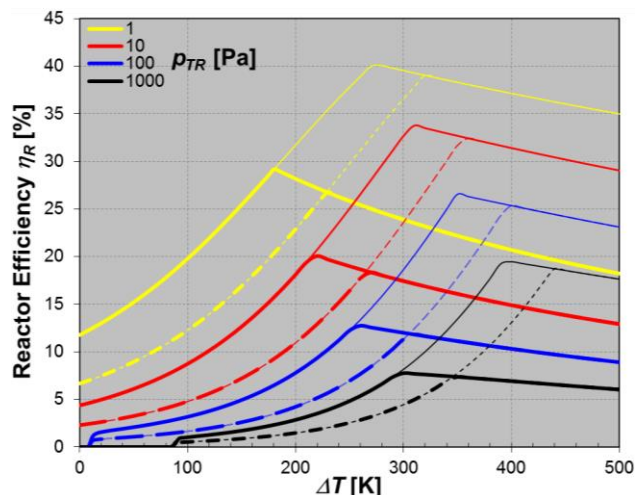


Figure 4. Calculated reactor efficiencies as a function of  $\Delta T$ . Solid lines are for  $\varepsilon_{GG}=0.8$ , whereas dashed lines are for  $\varepsilon_{GG}=0.6$ . Thick lines are for  $\varepsilon_R=0$ , and thin ones for  $\varepsilon_R=0.75$ . Lines of the same color correspond to the same  $p_{TR}$ .

A peak efficiency,  $\eta_R(\Delta T_{opt})$ , exists for any of the combinations of  $p_{TR}$ ,  $\varepsilon_R$ , and  $\varepsilon_{GG}$  in Fig. 4. For the chosen range of parameters,  $\Delta T_{opt}$  varies roughly between 180 K and 440 K. Furthermore, for most regimes, ITWS efficiency is several-fold lower than that at  $\Delta T_{opt}$ , and it also yields the lowest efficiency for all  $\varepsilon_R$  and  $\varepsilon_{GG}$ . This is especially pronounced for  $\varepsilon_{GG}=0.6$ . Other trends are also apparent. For example,  $p_{TR}$  decrease and  $\varepsilon_R$  decrease generally lead to a  $\Delta T_{opt}$  decrease, whereas  $\varepsilon_{GG}$  decrease leads to a  $\Delta T_{opt}$  increase. Efficiency generally increases with decreasing  $p_{TR}$ , and increasing  $\varepsilon_R$  and  $\varepsilon_{GG}$ . Conversely, the lowest efficiencies would be realized at high (e.g. atmospheric)  $p_{TR}$ , in the absence of heat recovery.

Some of the efficiency curves in Fig. 4 coincide. First, below  $\Delta T_{opt}(\varepsilon_R=0)$ ,  $\eta_R(\varepsilon_R=0)=\eta_R(\varepsilon_R=0.75)$ . Second, above  $\Delta T_{opt}(\varepsilon_{GG}=0.6)$ ,  $\eta_R(\varepsilon_{GG}=0.6)=\eta_R(\varepsilon_{GG}=0.8)$ . Finally, curves for  $p_{TR}$  and  $\varepsilon_R=0$  coincide with curves for  $10 \cdot p_{TR}$  and  $\varepsilon_R=0.75$ , below  $\Delta T_{opt}(p_{TR}, \varepsilon_R=0)$ . The first two coincidences result from the balance of energy requirements in the cycle, including those that lead to low isothermal efficiency, and can be understood by considering the interplay of factors that determine  $\Delta T_{opt}$ . First, we recall that the unrecovered sensible heat of the reduced oxide and the heat of the reoxidation reaction are used to preheat the steam feedstock to near  $T_{WS}$ , via the hot  $H_2O-H_2$  exhaust (Fig. 1). Furthermore, oxide reduction ( $Q_{TR}$ ), oxide heating ( $Q_{SH}$ ), and steam heating ( $Q_{H_2O}$ ) are by far the three largest energy requirements in the system (depending on  $\Delta T$ ). Of these,  $Q_{SH}$  and  $Q_{H_2O}$  can be considered parasitic, since they do not directly contribute to  $H_2$  production (whereas  $Q_{TR}$  does, with an efficiency given by  $HHV_{H_2}/Q_{TR}$ ).<sup>9</sup> Therefore, at the point where  $Q_{SH}$  and  $Q_{H_2O}$  are roughly balanced, the least amount of direct solar input is required for steam heating or the least amount of the oxide sensible heat has to be rejected, thus leading to peak efficiency.

The coinciding efficiencies in Fig. 4 can now be explained as follows: First, below  $\Delta T_{opt}$ ,  $Q_{H_2O}$  is the largest energy requirement *and* it requires direct solar input (in addition to preheating). Specifically, the region of coincidence, where  $\eta_R(\varepsilon_R=0)=\eta_R(\varepsilon_R=0.75)$ , corresponds to a situation in which direct solar input is required for steam heating irrespective of  $\varepsilon_R$ . More generally, below  $\Delta T_{opt}(\varepsilon_R=0)$ ,  $Q_{H_2O}$  is sufficiently large to make efficiency independent on  $\varepsilon_R$ .

The situation corresponds to a low and eventually zero 2<sup>nd</sup> right-hand term in eq. 5 (at  $\Delta T=0$ ), and a large 4<sup>th</sup> term.

In light of this, the reasons behind the very low efficiency for ITWS are straightforward: While no energy is needed to heat the oxide after the water splitting reaction ( $Q_{SH}=0$  in Fig. 1),  $Q_{H2O}$  is at its maximum, even with extensive preheating by the H<sub>2</sub>O-H<sub>2</sub> output. This is because, at  $\Delta T=0$ , both  $n_{w/h}$  and  $\Delta T_{I/O}$  are at their maximum values. Since  $Q_{SH,L}=0$ , virtually all of  $Q_{H2O}$  requires direct solar input. This dominant role of  $Q_{H2O}$  in ITWS (but not for  $\Delta T > \Delta T_{opt}$ ) also strongly cautions against omitting this energy requirement from efficiency calculations, as is sometimes done.<sup>8</sup>

Second, for  $\Delta T > \Delta T_{opt}$ , oxide heating is the largest energy requirement *and* it requires direct solar input (to the extent that  $\epsilon_R < 1$ ). In this region,  $Q_{H2O}$  is small, mainly because, at low  $T_{WS}$ , comparatively little steam is needed to oxidize ceria back to equilibrium ( $n_{w/h}$  is small), but also because  $\Delta T_{I/O}$  is smaller, compared to ITWS. Therefore,  $Q_{SH}/Q_{H2O} > 1$ . In fact, at  $\Delta T > \Delta T_{opt}$ ,  $Q_{AUX} < 0$ , necessitating heat rejection. Alternatively, this high quality waste heat can be used for other purposes, even though it cannot directly increase reactor efficiency. This corresponds to a small 4<sup>th</sup> right-hand term in eq. 5 (compared to the 2<sup>nd</sup> term).

Lastly, coinciding efficiency curves for  $\epsilon_R=0$  and  $\epsilon_R=0.75$  reflect the particulars of ceria thermodynamics. As it happens, below  $\Delta T_{opt}(p_{TR})$ , decreasing  $p_{TR}$  by a factor of 10 is equivalent, in efficiency terms, to increasing  $\epsilon_R$  from 0 to 0.75.

The high  $\epsilon_{GG}$  required for efficient ITWS and low  $\Delta T$  operation warrants some further consideration. High levels of gas-gas heat recovery (>97%) are attainable at temperatures up to roughly 923 K using stainless steel recuperators. At higher temperatures, creep and corrosion limitations require the use of nickel alloys (up to  $\approx 1273$  K), and no recuperators operating at 1773 K (or higher!) have been reported.<sup>26, 27</sup> Since in ITWS  $Q_{H2O}$  is the highest, the role of gas-gas heat exchange is critical. For ITWS at  $p_{TR}=1$  Pa,  $T_{iso}=1773$  K and  $\Delta T_{I/O}=1475$  K, nearly 100 mol of steam must be heated per mole of produced H<sub>2</sub> (Fig. 2a). The associated energy requirement considerably exceeds the chemical energy content of the H<sub>2</sub> product, even for high  $\epsilon_{GG}$ .

The above further underscores the challenges associated with ITWS: If an exceptionally high  $\epsilon_{GG}$  cannot be achieved in practice, the efficiencies for ITWS would be even lower than those shown in Fig. 4. On the other hand, as  $\Delta T$  increases (i.e.  $T_{WS}$  decreases), higher  $\epsilon_{GG}$  values become more realistic. To account for this, we calculate efficiency in a more flexible fashion, by using a variable  $\epsilon_{GG}$ , such that it is realistic at both high and low  $T_{WS}$  (Fig. 5).

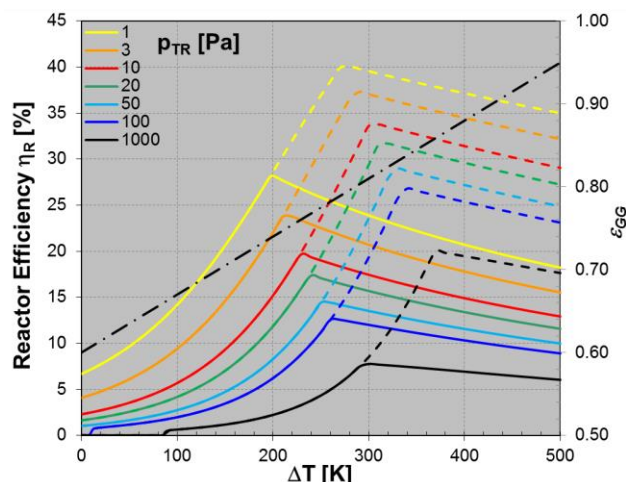


Figure 5. Calculated reactor efficiencies (left y-axis) as a function of  $\Delta T$ , for  $\varepsilon_{GG}$  linearly increasing from  $\varepsilon_{GG}(1773\text{ K})=0.6$  to  $\varepsilon_{GG}(1273\text{ K})=0.95$ . This roughly corresponds to a situation where heat from the output steam- $\text{H}_2$  mixture is rejected above 1273 K. Solid lines are for  $\varepsilon_R=0$ , dashed lines are for  $\varepsilon_R=0.75$ . The dash-dot line shows  $\varepsilon_{GG}$  on the right y-axis.

The results in Fig. 5 give insight into what might be expected in practice, and show an even larger efficiency advantage of TSWs over ITWS. Although this analysis is for a pumped reactor, it is worth repeating at this point that efficiently recovering heat from a sweep gas would face the same obstacles as in the case of steam, with the added construction difficulty that it must be performed at  $T_{TR}$ , irrespective of  $\Delta T$ . However, operating at  $\Delta T_{opt}$  and under best-case conditions, would significantly decrease sweep gas requirements compared to ITWS, thus much decreasing, possibly even eliminating the need for heat recovery from the inert-oxygen exhaust and associated hardware complications. An inert gas purification plant would still be necessary.

Solid-solid heat recovery being also challenging, we have consistently included the limiting case of  $\varepsilon_R=0$ . Understanding that  $\varepsilon_R=0.75$  is near the upper end of what may be possible in practice, plots such as that in Fig. 5 can be helpful for roughly estimating maximum reactor efficiency (for a  $\text{CeO}_2$  cycle): for every  $p_{TR}$ , it lies approximately between the peaks of the corresponding solid and dashed lines. The results in Figs. 4 and 5 in show that for ceria and moderate values of the operating parameters, such as  $p_{TR}>10\text{ Pa}$ ,  $\varepsilon_R<0.5$ , and  $\varepsilon_{GG}<0.7$ , efficiency ranges roughly from 10 to 25%, whereas the  $\Delta T_{opt}$  range is roughly between 250 K and 400 K.

It should be noted at this point that the assumption that all reactions end in their thermodynamic equilibrium states is more important in ITWS, when  $\Delta\delta$  is small and the system operates near equilibrium, than for  $\Delta T>0$ , when  $\Delta\delta$  is comparatively large. Therefore, any deviations from this assumption, as is certain to be the case in practice, would further disfavor ITWS.

In addition to maximizing efficiency for a given reactor/material system, knowing  $\Delta T_{opt}$  can guide reactor design. This is illustrated in Fig. 6, showing  $\eta_R(\Delta T_{opt})$  as function of  $p_{TR}$ , for several  $\varepsilon_R$  and  $\varepsilon_{GG}$ . It is evident that, for a ceria-based reactor operating at  $\Delta T_{opt}$ ,  $\varepsilon_R$  influences efficiency more than  $\varepsilon_{GG}$  does. For example, increasing  $\varepsilon_R$  from 0 to 0.5 allows the same efficiency to be achieved at a roughly 10 times higher  $p_{TR}$ . This type of plot can be used to help evaluate the cost of achieving a certain  $p_{TR}$ ,  $\varepsilon_R$ , or  $\varepsilon_{GG}$  vs. corresponding efficiency benefits.

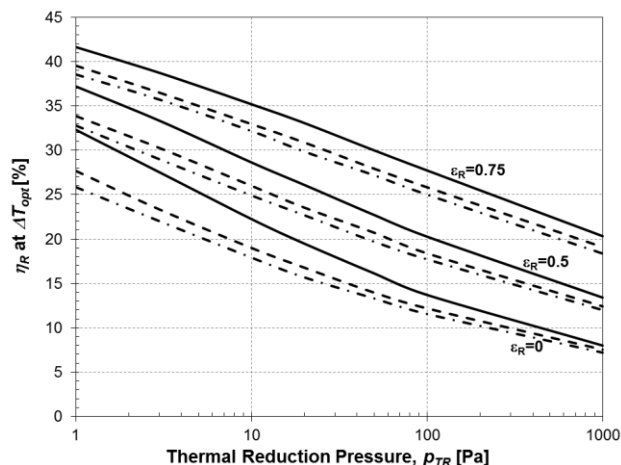


Figure 6. Calculated reactor efficiencies at  $\Delta T_{opt}$  (ranging from 130 K to 460 K) as function of  $p_{TR}$ . The three groups of lines correspond to three values of  $\epsilon_R$ . Within the groups, solid lines correspond to  $\epsilon_{GG}=0.9$ , dashed to  $\epsilon_{GG}=0.7$ , and dash-dot lines to  $\epsilon_{GG}=0.5$ .

#### 4. Discussion

As seen in Fig. 2a, a reactor producing  $H_2$  from  $H_2O$  in an isothermal two-step cycle, must operate at high thermal reduction temperatures, very low thermal reduction pressures, or at an exceptionally high  $n_{w/h}$ , or some combination of the three. These basic limitations are entirely a consequence of water thermodynamics and cannot be circumvented by any material discovery or innovative reactor design. High operating temperatures place extraordinary demands on reactor materials, and require unrealistically high concentration ratios from the solar collector and concentrator system. Low thermal reduction pressures require very large receivers and pumps – an undertaking of possibly prohibitive cost. Finally, high values of  $n_{w/h}$  make water near ambient temperature, not  $H_2$ , the main reactor product. This necessitates either high temperature  $H_2$  separation, or the addition of a high-throughput, high-efficiency steam heat recovery system, which preheats the input water while cooling the output steam- $H_2$  mix. Each of these factors complicate reactor and plant design and compromise economics: Therefore, when the entire balance of plant is considered, ITWS makes matters more difficult, not easier, as one might hope.

Further, in addition to posing extraordinary design and operational demands, ITWS offers no efficiency payoff. On the contrary, it appears to be the most inefficient fashion of producing  $H_2$  from  $H_2O$  in a two-step cycle (Figs. 3 and 4). Even in the most favorable case, without solid-solid heat recovery, ITWS with a high level of steam-steam heat recovery ( $\epsilon_{GG}=0.8$ ), is less efficient than TSWS at  $\Delta T_{opt}$  for a far more plausible  $\epsilon_{GG}=0.6$  (Fig. 4). This disadvantage only widens for  $\epsilon_R > 0$  or when a realistic  $T_{WS}$ -dependent  $\epsilon_{GG}$  is included (Figs. 4 and 5).

Recalling that the question in solar fuel production is not one of feasibility, but of efficient solar utilization and minimization of the product cost, no ITWS advantages are evident in our analysis. Rather, requiring that  $T_{TR}=T_{WS}$  seems to be an unnecessary and counterproductive limitation. On the other hand, TSWS at  $\Delta T_{opt}$  maximizes solar resource utilization, and the associated low steam requirement simplifies plant design and operation.

The very existence of  $\Delta T_{opt}$  may seem peculiar if one thinks of thermochemical reactors as engines that reverse combustion, i.e. where heat is the input and fuel (chemical work) is the output. It may initially appear most plausible that maximizing  $\Delta T$  would also maximize

efficiency. In the case of perfect heat recovery ( $\varepsilon_R = \varepsilon_{GG} = 1$ ), this would be correct. It is because of the reality of non-ideal heat recovery that  $\Delta T_{opt}$  exists at all.

Some general implications regarding reactor operation follow from the above results. Under all conditions, the slopes of the efficiency curves are shallower for  $\Delta T > \Delta T_{opt}$  than for  $\Delta T < \Delta T_{opt}$ . Furthermore, the reasons for suboptimal efficiency are different in these two regions. For  $\Delta T > \Delta T_{opt}$ , the oxide heating requirement results in the production of high quality waste heat (at  $T_{WS}$ ), which can be used elsewhere in the plant, even if not for  $H_2$  production directly. For  $\Delta T < \Delta T_{opt}$ , however, efficiency decreases because of the steam heating requirement, with waste heat available at low temperature (following steam-steam heat recovery) and of little value. This suggests that it may be prudent to err on the side of  $\Delta T > \Delta T_{opt}$ , rather than the opposite, in order to achieve higher average efficiency under the variable environmental conditions present in practice.

Even though the feasibility of thermochemical fuel production using ceria as a working oxide has been demonstrated,<sup>24, 28, 29</sup> a consensus exists regarding the need for material improvements. Most notable of them is the need for a material that provides a higher  $\Delta\delta$  at a higher  $p_{TR}$  and lower  $T_{TR}$  than, for example, ceria, yet with similar kinetics and stability. In addition to the possibility of less demanding operation (at a lower required  $T_{TR}$ ), a higher  $\Delta\delta$  would enable higher yields, so that less oxide must be heated per unit produced  $H_2$  or fuel in general. Importantly, this increase must not be offset by an equal increase in  $C_p$  or more precisely  $C_p\Delta T$  (cf. eq. 10 and compare, for example,  $C_p$  for ceria with that of  $LaMnO_3$  or  $La_{1-x}Sr_xMnO_3$ ).<sup>22, 30-32</sup> A material that reduces more easily than ceria (larger  $\delta$  under identical  $T_{TR}$  and  $p_{TR}$ ) will generally also be more difficult to reoxidize, assuming similar and temperature independent values for  $\Delta S$ . This assumption is justified as  $\Delta S$  is largely a function of the evolution of oxygen into the gas phase.<sup>33</sup> Operationally, this suggests that advanced materials may require a lower  $T_{WS}$  (larger  $\Delta T$ ) for reoxidation to achieve the same  $n_{w/h2}$ . In other words, an insufficiently large  $\Delta\delta/C_p$  increase could be offset by an increase in the 2<sup>nd</sup> right-hand term in eq. 5, and therefore decrease efficiency.

Understanding this, it is to be expected that optimal operation with advanced materials is likely to involve an increase of  $\Delta T_{opt}$ , not its decrease in the direction of ITWS. Precise details would additionally depend on reactor design and various internal efficiencies such as  $\varepsilon_R$ ,  $\varepsilon_{GG}$ , etc. This also follows from general thermodynamic consideration regarding the maximum theoretical efficiency of a two-step thermochemical process.<sup>5</sup> Because of strict thermodynamic limitations, ITWS is unlikely to benefit from the use of advanced materials.

While some key design and operating parameters of a thermochemical reactor for two-step  $H_2$  production present obvious tradeoffs between difficulty and efficiency,  $\Delta T$  is not one of them. For example, the higher the degree of heat recovery ( $\varepsilon_R$  or  $\varepsilon_{GG}$ ), which is increasingly difficult to accomplish, the higher the efficiency. One must therefore find a balance that minimizes the levelized cost of the  $H_2$  product. The choice of  $\Delta T$  is easier to make: operating difficulty being largely independent of  $\Delta T$ , it would always be advantageous to operate at  $\Delta T$  for which efficiency is the highest.

Finally, we note that even though much of this analysis is specific to  $CeO_2$  as a reactive oxide, it can be applied to any material for which sufficient thermodynamic information is available. With appropriate small adaptations (mainly heat capacity and dissociation coefficients), the analysis can also be applied to the solar-thermochemical production of CO from  $CO_2$ , with largely the same conclusions.

#### 4. Conclusions

The conditions ( $T_{iso}$ ,  $p_{O_2}$  and  $n_{w/h}$ ) required for isothermal two-step thermochemical water splitting ( $T_{TR}=T_{WS}$ ) can be determined based on water thermodynamics and are highly mutually dependent: choosing values for any two defines the third. This analysis shows that isothermal water splitting is impractical, being a choice between high thermal reduction temperatures, very low oxygen partial pressures for thermal reduction, or exceptionally high steam requirements (i.e. high separation work) – or some combination of the three.

Isothermal water splitting is substantially less efficient than the same process at  $\Delta T > 0$ . This is true even in the complete absence of solid-solid heat recovery in the latter case, *and* assuming a high steam heat recovery effectiveness at high temperature. The low efficiency of ITWS is primarily a result of the exceptionally high energy requirement for steam heating in the water splitting step of the cycle.

Given a specific reactor/material combination, an optimal  $\Delta T = T_{TR} - T_{WS}$  can be found to maximize efficiency. For reasonable values of process parameters in a ceria-based cycle, this  $\Delta T_{opt}$  ranges roughly between 250 K and 400 K, and is expected to increase in well-designed advanced materials.

A combination of pressure and temperature swing, rather than either individually, is by a wide margin the most efficient mode of operation of a two-step cycle thermochemical reactor for hydrogen production. Efficiency being of paramount importance for the practical application of this technology, temperature and pressure swing reactors appear to be the most promising direction for future research and development.

#### Acknowledgements

The authors would like to thank Dr. T. M. Besmann of Oak Ridge National Laboratory, who provided the  $CeO_{2-x}$  model, based on data from Zinkevich et al.<sup>20</sup> Many useful discussions with Anthony McDaniel of Sandia National Laboratories and Nathan Siegel of Bucknell University are gratefully acknowledged as well. This work was supported by the U.S. Department of Energy Fuel Cell Technologies Program via the Solar Thermochemical Hydrogen (STCH) directive, and the Advanced Materials for Next Generation High Efficiency Thermochemistry LDRD project. Sandia is a multiprogram laboratory operated by Sandia Corporation, a Lockheed Martin Company, for the United States Department of Energy's National Nuclear Security Administration under Contract DE-AC04-94AL85000.

#### References

1. R. B. Diver, J. E. Miller, M. D. Allendorf, N. P. Siegel and R. E. Hogan, *Journal of Solar Energy Engineering*, 2008, 130, 041001-041001 -041001-041008.
2. E. B. Stechel and J. E. Miller, *Journal of CO2 Utilization*, 2013, 1, 28-36.
3. J. Kim, T. A. Johnson, J. E. Miller, E. B. Stechel and C. T. Maravelias, *Energy & Environmental Science*, 2012, 5, 8417-8429.
4. N. P. Siegel, J. E. Miller, I. Ermanoski, R. B. Diver and E. B. Stechel, *Industrial & Engineering Chemistry Research*, 2013, 52, 3276-3286.
5. J. E. Miller, A. H. McDaniel and M. D. Allendorf, *Advanced Energy Materials*, 2013, DOI: 10.1002/aenm.201300469, 1-19.
6. R. Bader, L. J. Venstrom, J. H. Davidson and W. Lipiński, *Energy & Fuels*, 2013, 27, 5533-5544.
7. Y. Hao, C.-K. Yang and S. M. Haile, *Physical Chemistry Chemical Physics*, 2013, 15, 17084-17092.
8. C. L. Muhich, B. W. Evanko, K. C. Weston, P. Lichty, X. Liang, J. Martinek, C. B. Musgrave and A. W. Weimer, *Science*, 2013, 341, 540-542.

9. I. Ermanoski, N. P. Siegel and E. B. Stechel, *Journal of Solar Energy Engineering*, 2013, 135, 031002-031001 - 031010.
10. R. J. Panlener, R. N. Blumenthal and J. E. Garnier, *Journal of Physics and Chemistry of Solids*, 1975, 36, 1213-1222.
11. Y. Du, M. Yashima, M. Kakihana, T. Koura and M. Yoshimura, *J. Am. Ceram. Soc.*, 1994, 77, 2783-2784.
12. M. Foex, *Rev. Int. Hautes Temp. Refract.*, 1966, 3, 309-&.
13. R. J. Fruehan, *Metallurgical Transactions B-Process Metallurgy*, 1979, 10, 143-148.
14. S. A. Gallagher and W. R. Dworzak, *J. Am. Ceram. Soc.*, 1985, 68, C206-C207.
15. Blumenth.Rn and R. L. Hofmaier, *J. Electrochem. Soc.*, 1974, 121, 126-131.
16. E. J. Huber and C. E. Holley, *J. Am. Chem. Soc.*, 1953, 75, 5645-5647.
17. M. E. Huntelaar, A. S. Booij, E. H. P. Cordfunke, R. R. van der Laan, A. C. G. van Genderen and J. C. van Miltenburg, *J. Chem. Thermodyn.*, 2000, 32, 465-482.
18. B. Iwasaki and T. Katsura, *Bull. Chem. Soc. Jpn.*, 1971, 44, 1297-&.
19. B. H. Justice and E. F. Westrum, *J. Phys. Chem.*, 1969, 73, 1959-&.
20. M. Zinkevich, D. Djurovic and F. Aldinger, *Solid State Ionics*, 2006, 177, 989-1001.
21. H. Lukas, S. G. Fries and B. Sundman, *Computational Thermodynamics: The Calphad Method*, University Press, Cambridge, 2007.
22. M. Ricken, J. Nölting and I. Riess, *Journal of Solid State Chemistry*, 1984, 54, 89-99.
23. K. N. Marushkin, K. V. B. and A. S. Alikhanyan, *Inorganic Materials*, 2000, 36, 793-798.
24. S. Abanades and G. Flamant, *Solar Energy*, 2006, 80, 1611-1623.
25. K. Z. House, A. C. Baclig, M. Ranjan, E. A. van Nierop, J. Wilcox and H. J. Herzog, *Proc. Natl. Acad. Sci. U. S. A.*, 2011, 108, 20428-20433.
26. P. J. Maziasz and R. W. Swindeman, *Journal of Engineering for Gas Turbines and Power*, 2002, 125, 310-315.
27. J. Min, J. Jeong, M. Ha and K. Kim, *Heat Mass Transfer*, 2009, 46, 175-186.
28. W. C. Chueh, C. Falter, M. Abbot, D. Scipio, P. Furler, S. Haile and A. Steinfeld, *Science*, 2010, 330, 1797-1800.
29. J. E. Miller, M. D. Allendorf, A. Ambrosini, E. N. Coker, R. B. Diver, I. Ermanoski, L. R. Evans, R. E. Hogan and A. McDaniel, *Development and Assessment of Solar-Thermal-Activated Fuel production: Phase 1 Summary*, Report SAND2012-5658, Sandia National Laboratories, Albuquerque, New Mexico, 2012.
30. K. T. Jacob and M. Attaluri, *Journal of Materials Chemistry*, 2003, 13, 934-942.
31. A. H. McDaniel, E. C. Miller, D. Arifin, A. Ambrosini, E. N. Coker, R. O'Hayre, W. C. Chueh and J. Tong, *Energy & Environmental Science*, 2013, 6, 2424-2428.
32. A. Szewczyk, M. Gutowska and B. Dabrowski, *Physical Review B*, 2005, 72, 224429.
33. B. Meredig and C. Wolverton, *Physical Review B*, 2009, 80, 245119.